Cyclic MOG$_{35–55}$ ameliorates clinical and neuropathological features of experimental autoimmune encephalomyelitis

Cyclic MOG_{35-55} ameliorates clinical and neuropathological features of experimental autoimmune encephalomyelitis

Athanasios Lourbopoulos [a], George Deraos [b], Minos-Timotheos Matsoukas [c], Olga Touloumi [a], Aggeliki Giannakopoulou [a], Hubert Kalbacher [d], Nikolaos Grigoriadis [a,*], Vasso Apostolopoulos [e,*], John Matsoukas [f,*]

[a] *Laboratory of Experimental Neurology and Neuroimmunology, B' Department of Neurology, AHEPA University Hospital, Thessaloniki, Greece.*
[b] *Department of Chemistry, University of Patras, Patras 26500, Greece*
[c] *Department of Pharmacy, University of Patras, Patras 26500, Greece*
[d] *Interfaculty Institute of Biochemistry, University of Tubingen, Tubingen, Germany*
[e] *Centre for Chronic Disease, College of Health and Biomedicine, Victoria University, VIC 3030 Australia*
[f] *Eldrug, Patras Science Park, Patras, Greece.*

Running Title: Cyclic MOG_{35-55} ameliorates EAE

Abbreviations: CFA, complete Freund's adjuvant; cMOG, cyclic MOG_{35-55} peptide; c-MOG_{35-55}, cyclic MOG_{35-55} peptide; CNS, central nervous system; HLA, human leukocyte antigen; l-MOG_{35-55}, linear MOG_{35-55} peptide; MBP, myelin basic protein; MHC, major histocompatibility complex; MOG, myelin oligodendrocyte glycoprotein; MS, multiple sclerosis; TCR, T cell receptor

* Corresponding authors and equal contribution:
Email addresses:
vasso.apostolopoulos@vu.edu.au (V.Apostolopoulos)
imats@upatras.gr (J. Matsoukas)
grigoria@med.auth.gr (N. Grigoriadis)

ABSTRACT

EAE is induced to susceptible mice using linear peptides of myelin proteins of the central nervous system. Specific peptide motifs within the peptide-binding groove of the MHC peptide-complex determines the affinity of the peptide in each animal and the consequent T-cell receptor recognition and activation of the cell. Altered peptide ligand (APL) vaccination is a novel approach based on an effort to induce T-cell tolerance or alter cytokine profile from pro-inflammatory to anti-inflammatory. In the present study we synthesized the MOG_{35-55} peptide and altered its 3-dimensional conformation to make it a cyclic one (c-MOG_{35-55}). EAE was induced in C57BL/6 mice and pathology was studied on acute and chronic phase of the disease. Our data indicates that c-MOG_{35-55} peptide alone induces a mild transient acute phase without chronic axonopathy. Administration of the c-MOG_{35-55} peptide at a 1:1 ratio during disease induction significantly ameliorates clinical disease and underlying pathology, such as demyelination and axonopathy in the acute and chronic phases. Binding and structural studies revealed milder interactions between the c-MOG_{35-55} and mouse or human MHC class II alleles ($H2\text{-}IA^b$ and HLA-DR2). Collectively, we provide data supporting for the first time the concept that the cyclic modification of an established encephalitogenic peptide ameliorates the clinical outcomes and underlying pathological processes of EAE. Such a cyclic modification of linear peptides could provide a novel treatment approach for future, patient-selective, immunomodulative treatments of multiple sclerosis.

Keywords:
Experimental autoimmune encephalomyelitis
Multiple sclerosis
Cyclic peptide
Myelin oligodendrocyte glycoprotein

1. Introduction

Multiple sclerosis (MS) is defined as a chronic, demyelinating disease of the central nervous system,[1] where immune cells (macrophages, T helper (h)1, Th2, Th17, CD8+ T cells, B cells) migrate to the site of damage (the myelin sheath) and induce inflammation, demyelination and neurodegenaration.[1] The recognition of self myelin peptides by $CD4^+$ T cells that are presented by the major histocompatibility complex (MHC) class II is one of the processes involved in the pathogenesis of multiple sclerosis (MS). Auto reactive $CD4^+$ T cells to self antigen, myelin basic protein (MBP) residues 83-99 (MBP_{83-99}) in complex with HLA-DR2 (DRA, DRB1*1501) in humans is associated with susceptibility to MS.[2-4] As a consequence, autoreactive $CD4^+$ T cells secrete Th1 cytokines such as, IL-1, IL-6, IFN-γ and TNF-α inducing an inflammatory mileau.[5] Other constituents of myelin that are important in the myelination of nerves and are targets for autoimmune attack are, myelin oligodendrocyte glycoprotein (MOG) and proteolipid protein (PLP).

A number of studies have shown anti-MOG antibodies to be involved in the pathogenesis of MS.[6] In addition, high T cell precursor frequencies against MOG have been noted patients with MS, in particular to MOG epitopes, MOG_{1-22}, MOG_{34-56} and MOG_{64-96} supporting a primary role of auto-immune $CD4^+$ T cells to MOG in disease development; although high levels of T cells against MOG are also noted in healthy individuals.[7-9] Of interest, T cells isolated from HLA-DR2 positive MS patients reacted to MOG peptides by secretion of high IFN-γ but not by T cells from healthy individuals, suggesting a role of HLA-DR2 in disease.[10] In fact, $HLA\text{-}DR2^+$ and $HLA\text{-}DR4^+$ (DRB1*0401) asrtocytes and microglia effectively present MOG epitopes to $CD4^+$ T cells inducing mixed Th1/Th2 cytokine responses, whereas MOG epitope presentation by dendritic cells induce predominantly Th1 cytokines.[11] Of relevance, in HLA-DR2 transgenic mice murine MOG_{35-55} was noted to be strongly immunogenic and induced experimental autoimmune encephalomyelitis (EAE) whilst human MOG_{35-55} (differs by one amino acid of P^{42} instead of S^{42}) was immunogenic but not encephalitogenic. These findings paved the way to studying MOG_{35-55} peptide as a potential pathogenic determinant in humans with MS.[12]

EAE is an experimental model of demyelination, inflammatory processes and axonopathy within the central nervous system (CNS) of susceptible animals, using the triggering of various CNS antigens such as MBP, PLP and MOG proteins or their peptides.[13, 14] Due to the similarities of EAE with MS, this model is widely used to study pathological mechanisms as well as novel experimental treatments for the disease. EAE is induced to susceptible animals using linear peptides (antigens) of myelin proteins of the CNS. These peptides bear different antigenic properties in each animal species and disease is determined by the properties of the MHC class II haplotype of the animal. In fact, injection of C57BL/6 mice with the linear peptide of MOG_{35-55} (l-MOG_{35-55}) suspended in complete Freund's adjuvant (CFA) followed by 2 pertussis toxin injections, develop a classic self-limiting monophasic EAE with ascending flaccid paralysis within 2 weeks following injection and mice are usually monitored up to 50 days, depending on the severity of EAE symptoms.[15] The interaction between the peptide, MHC class II and the T cell receptor (TCR) forming a trimolecular complex is the key to disease induction. Any modification to the antigenic peptide and any caused deviation from a tight MHC class II-peptide-TCR complex can lead to reduced T-cell activation, T cell anergy and/or different cytokine profiles.[16-18] Based on this concept, there have been several attempts to alter the trimolecular complex affinities and render autoreactive T-cells in MS and EAE inactive,

altered or eliminated. This approach has utilized either T-cell vaccination, T-cell receptor peptide vaccination, DNA vaccination or altered peptide ligand (APL) vaccination.[18-26]

In the present study we used a rather different therapeutic approach to ameliorate EAE in C57BL/6 mice. We synthesized the immunogenic and encephalitogenic MOG_{35-55} peptide (l-MOG_{35-55}) and altered its 3D conformation to make it a cyclic one (c-MOG_{35-55}). In this way we kept the same antigenic linear epitope of MOG_{35-55} but changed the sterotaxy of the molecule so as to reduce the affinity and proximity of the TCR with the MHC in the trimolecular complex. This is the first time, according to our knowledge, that such a chemical conformation of the linear MOG_{35-55} is reported. Using binding studies and molecular modeling of c-MOG_{35-55} to human (HLA-DR2) and mouse (H2-IA^b) MHC class II molecules, we also provide computational data on how such a cyclic conformation could affect TCR-MHC affinity. As an *in vivo* proof-of-concept experimental study, we tested the possible encephalogenity of this newly synthesized c-MOG_{35-55} peptide in the C57BL/6 mice and used the peptide as a preventive treatment in the corresponding l-MOG_{35-55} model of EAE. In the induced EAE both clinical course and pathology were studied.

The development of cyclic molecules that mimic the immunomodulatory activity of myelin linear epitopes, while maintaining an advantage over regular peptides in regards to its stability, is a necessary step prior to these molecules being proposed as drug leads. The use of cyclic peptides instead of linear counterparts as therapeutic entities has a number of advantages, such as (i) stability and resistance to enzymatic degradation, (ii) improved receptor selectivity, resulting in an improved pharmacological profile, (iii) defined conformation allowing identification of active sites and, (iv) design of useful templates for the development of a non-peptide (mimetic) drug for oral administration. We previously described the rational design and synthesis of a number of cyclic peptides, based on a combination of conformational analysis studies and theoretical calculations carried out on the linear MBP peptides using 2D NOESY and ROESY NMR spectroscopy.[17, 19-22, 27-31]

2. Results and discussion

2.1. c-MOG_{35-55} is mildly immunogenic and ameliorates l-MOG_{35-55} (control) EAE

In order to test the *in vivo* immunogenic effects of c-MOG_{35-55} on EAE in mice, mice were injected with c-MOG_{35-55} peptide alone (immunogenicity) or in a 1:1 emulsion with the l-MOG_{35-55} peptide (preventive treatment; 1:1 c-MOG_{35-55}:l-MOG_{35-55} peptide).

Our data indicate that c-MOG_{35-55} ameliorates both chronic and acute phase of EAE (Fig. 1). In the chronic experiments, mice developed moderate EAE with slow and relatively delayed disease onset (the clinical course of the chronic EAE is presented in Fig. 1A). No animals died from EAE in either group. The overall disease burden, as defined by the mean Areas Under the Curve (mAUC, Fig. 1B), for each group was significantly lower in group B (mAUC = 39.63 ± 7.12) compared to control group mAUC = 68.72 ± 11.07, p=0.036). The mean clinical score was statistically significantly different at days 21-28, 30-34 and 46 (p<0.05). The maximal disease burden (as defined by Mean Maximal Clinical Scores, MMS) was significantly lower in treated group as compared to controls (control MMS = 3.3 ± 0.42 and group B MMS = 2.13 ± 0.34, p=0.043, Fig. 1C). Both groups had a similar day of disease onset (dDO), defined

as the first day with clinical score of “1”, (control = 17.90 ± 3.17 and group B = 21.90 ± 3.32; Kaplan-Meier survival analysis, log rank p=0.358, Fig. 1D).

Experiments of the acute phase of EAE replicated the main acute clinical findings of chronic experiments, importantly under a more severe, more aggressive and faster disease background (Fig. 1E). By definition, all mice were sacrificed 5 days post their first clinical sign of EAE (i.e on day 16, acute phase). No animals died in either group, until the day of sacrifice. The burden of disease for the acute phase (mAUC, Fig. 1F) was lower for group B (treated) compared to control (group B mAUC = 7.62 ± 2.09, control group mAUC = 18.56 ± 1.46, p=0.01). Treated mice had lower mean clinical scores from day 11 onwards (p<0.05 for day 11, p<0.01 for days 14-16). The maximal disease burden (MMS) was not calculated for this experiment because mice were not followed-up long enough to reach their maximal scores. Again, both groups had almost similar day of disease onset (mean dDO for control = 11.67 ± 0.49 and group B = 13.67 ± 0.84; Kaplan-Meier survival analysis, log rank p=0.073, Fig. 1G).

Injection with the c-MOG_{35-55} alone showed a mild encephalitidogenic potential for the peptide, that is not sustained long-term. Mice injected with c-MOG_{35-55} peptide alone developed a mild disease, with one mild acute phase and minimal residual chronic deficits, compared to a severe chronic EAE of control animals (p<0.01 for days 14 onwards, Fig. 1H). The total disease burden by c-MOG_{35-55} was minimal in most mice (c-MOG_{35-55} mAUC = 29.45 ± 14.87, control group mAUC = 109.29 ± 17.83, p=0.002, Fig. 1I). Although mice developed some mild to moderate disease symptoms (c-MOG_{35-55} MMS = 1.5 ± 0.48, control group MMS = 3.30 ± 0.47, p=0.033, Fig. 1J), these were not sustained long-term, suggesting a long-term disease resolution with minimal or no residual deficits. Disease onset was statistically similar in both groups (c-MOG_{35-55} and l-MOG_{35-55}, Kaplan-Meier survival analysis log-rank test p=0.0629), despite the fact that c-MOG_{35-55} mice had a trend for delayed disease onset (Fig. 1K).

Taken together, the clinical data suggests that injection with c-MOG_{35-55} has a very low encephalitogenic potential. However, the addition of c-MOG_{35-55} in the immunizing emulsion of EAE (l-MOG_{35-55}) ameliorates the overall disease burden and maximal clinical deficits, suggesting a preventative or immunomodulative effect for c-MOG_{35-55} peptide.

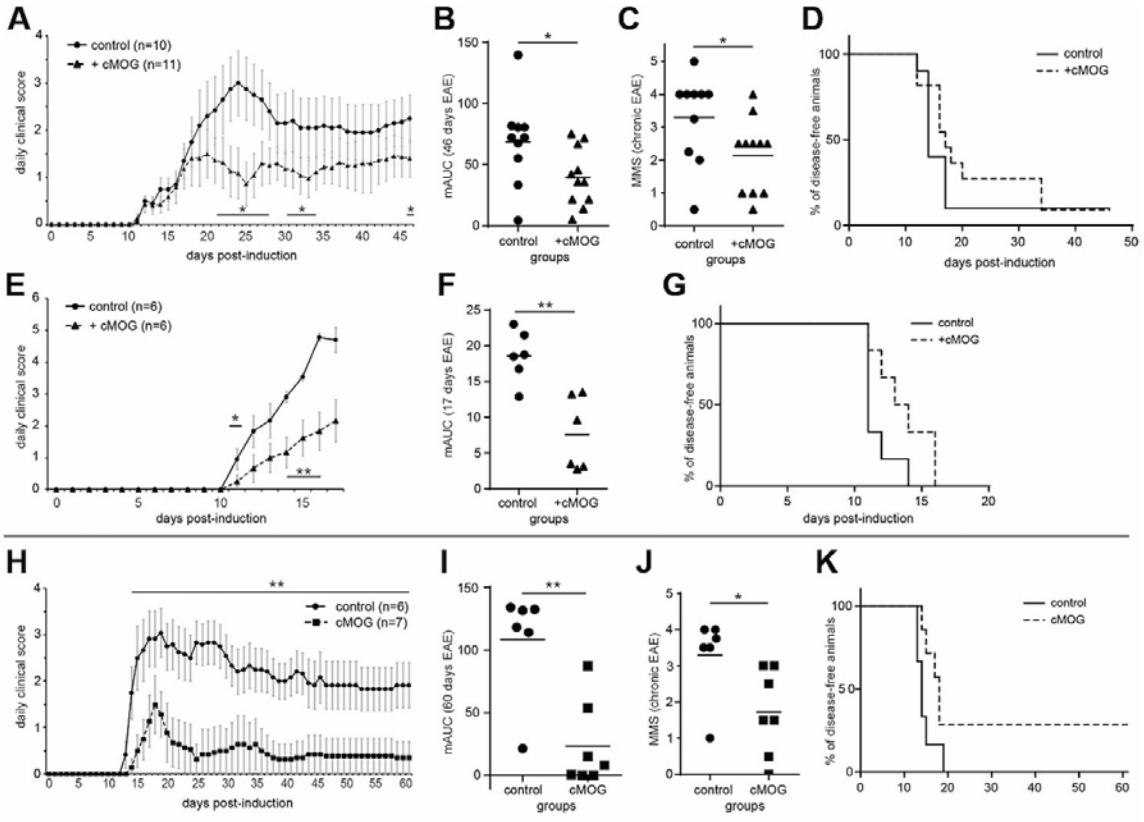

Fig. 1. Clinical course and outcome parameters of EAE with or without c-MOG$_{35-55}$. Panels (A-D) show the long-term (chronic) clinical course and parameters of animals co-immunized with the c-MOG$_{35-55}$ peptide (+cMOG): (A) the long-term follow-up of the disease, (B) the overall burden of disease (mAUC), (C) the maximal disease deficits (MMS) and (D) Kaplan-Meier survival analysis for the disease onset (% disease free animals). Panels (E-G) show the corresponding short-term (acute) clinical course and parameters of animals co-immunized with the c-MOG$_{35-55}$ peptide (+cMOG): (E) short-term follow-up, (F) burden of the disease and (G) survival analysis for the disease onset. Panels (G-J) show the long-term clinical course and parameters of animals immunized only with the c-MOG$_{35-55}$ peptide (cMOG) compared to controls (immunized with the l-MOG$_{35-55}$): (G) the long-term follow-up of the disease, (H) the overall burden of disease, (I) the maximal disease deficits and (J) survival analysis for the disease onset. Control groups in all EAE experiments are immunized with the l-MOG$_{35-55}$ peptide. * denotes p<0.05, ** p<0.01. Data of EAE cliical scores (A, E, G) are displayed as mean ± standard deviation (SD); horizontal lines in dot plots show means.

2.2. Histopathological evaluation

2.2.1. Co-immunization with c-MOG$_{35-55}$ reduces inflammatory processes of EAE

Study of inflammatory processes at acute and chronic phase of EAE showed that c-MOG$_{35-55}$ ameliorated the inflammatory processes of EAE. More specifically, during the acute phase, c-MOG$_{35-55}$reduced the total number of infiltrating cells per mm^2 (control group 260.51 ± 19.30, group B 172.23 ± 18.91, p=0.001, Fig. 2) and the size of inflammatory foci (inflammatory cells per infiltration: control group 55.75 ± 3.90, group B 37.61 ± 3.25, p<0.001). As a result, the chronic residual inflammatory burden (number of infiltrating cells per mm^2 (control group 28.14 ±4 .67, group B 14.36 ± 3.13, p=0.015, Fig. 3) and the size of inflammatory foci (control group 15.76 ± 2.34, group B 7.54 ± 1.27, p=0.002) were also ameliorated by the c-MOG$_{35-55}$.

Taken together, these data indicate that c-MOG$_{35-55}$ ameliorates the acute inflammatory processes within the spinal cords of the mice, which reflects to a reduced inflammatory burden long-term.

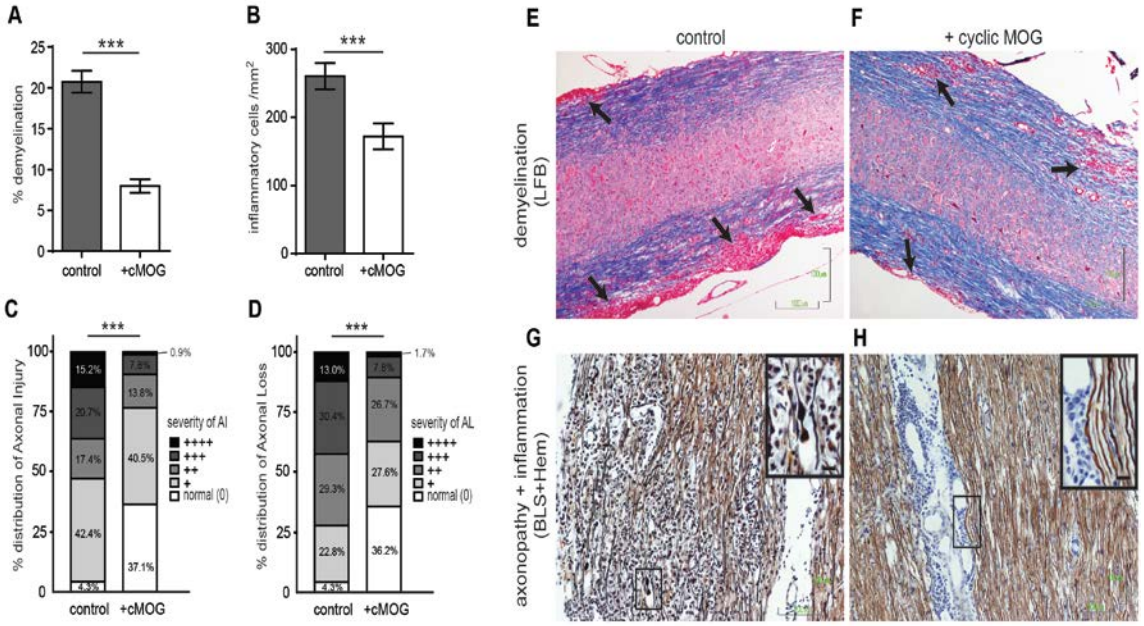

Fig. 2. (A) Demyelinating, (B) inflammatory and (C,D) axonopathic processes of control and +cMOG groups during the acute phase of EAE, in spinal cords. Graphs C and D show the axonal injury (AI) and loss (AL) as a semiquantitative distribution of severity (scales 0 to ++++ on the right side of graphs). Photos E and F show representative longitudinal spinal cord sections (under 10x objective) of a control and +cMOG co-immunized animal stained with LFB (blue: intact myelin, red: cell nuclei; arrows point at sites of inflammatory foci and/or demyelination). Note the more pronounced inflammation and demyelination of control mice. Photos G-H show representative longitudinal spinal cord sections (under 10x objective) of a control and +cMOG co-immunized animal stained with Bielschowsky and Hematoxylin (BLS+Hem) for axonopathy and inflammation (blue: cells bodies, dark brown: axons); inserts show magnifications of a cut axon in a control animal (spheroid/ovoid, insert of G) or intact axons next to inflammatory cells in +cMOG co-immunized animal (insert of H). *** denotes p<0.001. Data are displayed as mean ± standard error of the mean (SEM)

2.2.2. Co-immunization with c-MOG$_{35-55}$ reduces axonopathy and demyelination of EAE

Study of axonal pathology revealed a significant effect of c-MOG$_{35-55}$ treatment on axonal injury and loss. During acute phase, co-immunization with c-MOG$_{35-55}$ resulted in reduced axonal injury (AI) and axonal loss (AL) compared to control (Pearson's chi-square tests, p<0.001, Fig. 2C-D, G-H). During chronic phase, axonal loss was less in the mice co-immunized with c-MOG$_{35-55}$, compared to control (Pearson's chi-square test, p=0.001, Fig. 3D, G-H), reflecting an long-term axonal protection from c-MOG$_{35-55}$ peptide. Active axonal injury during the chronic phase (presence of dystrophic or cut axons, depicted as "pearls-strings" and "ovoids/spheroids" morphology; inserts in Fig. 3C, G-H) was also ameliorated in mice co-immunized with c-MOG$_{35-55}$ compared to controls, although this was marginally not statistically different (Pearson's chi-square test, p=0.071).

Studies of demyelination (on sections stained with LFB) showed that co-immunization with c-MOG$_{35-55}$ reduced the demyelinating area during acute phase, compared to controls (control group = 20.73 ± 1.34 and group B = 7.99 ± 0.83, p<0.001, Fig. 2A, E-F). The same beneficial effect of c-MOG$_{35-55}$ was also noted during the

chronic phase of the disease (control group = 14.92 ± 0.92 and group B = 6.77 ± 0.67, p<0.001) (Fig. 3A, E-F).

Taken together, these data indicate that c-MOG$_{35-55}$ significantly reduces the demyelinating and axonopathic processes of EAE during the acute phase of the disease, resulting in better anatomical integrity of the white matter tracts of the spinal cord. Importantly, this beneficial effect is maintained up to the chronic phase of the disease and is reflected to better neurological scores for the treated group

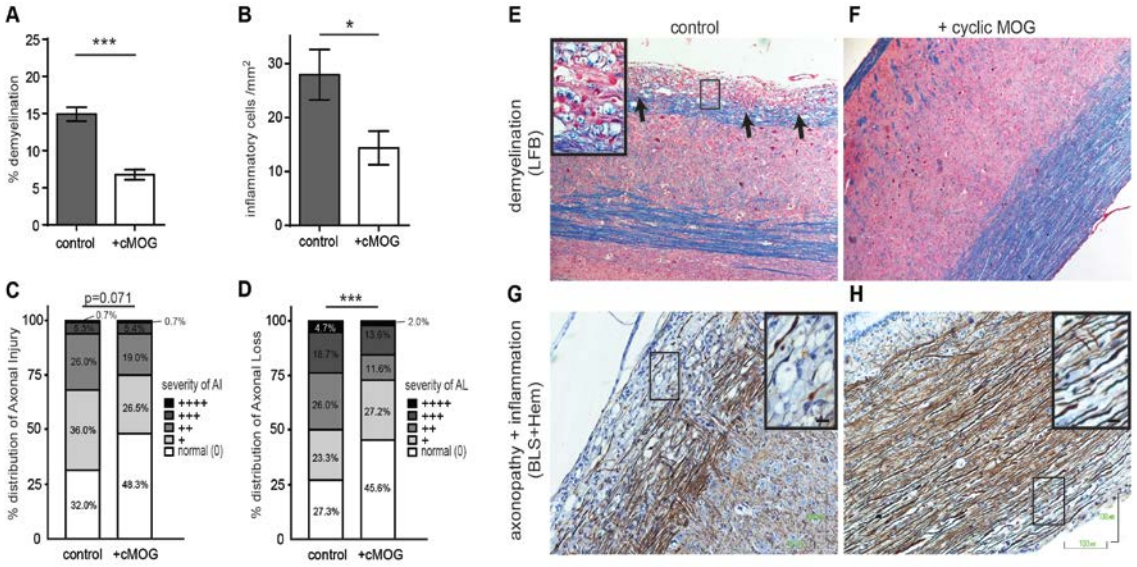

Fig. 3. (A) Demyelinating, (B) inflammatory and (C,D) axonopathic processes of control and +cMOG groups during the chronic phase of EAE, in spinal cords. Graphs C and D show the results of axonal injury (AI) and loss (AL) as a semiquantitative distribution of severity. Photos E and F show representative longitudinal spinal cord sections (under 10x objective) of a control and +cMOG co-immunized animal, stained with LFB (blue: intact myelin, red: cell nuclei; arrows point at sites of inflammatory foci and/or demyelination). Note the residual inflammation and pronounced demyelination of control mice with presence of vacuolation and myelin debris (blue staining within vacuoles or cells, insert in e). Photos G-H show representative longitudinal spinal cord sections (under 10x objective) of a control (G) and +cMOG co-immunized (H) mice stained with BLS+Hem for axonopathy and inflammation (blue: cells bodies, dark brown: axons); inserts show magnifications of an area with severe axonal loss and ongoing injury in a control animal (almost complete absence of dark brown axons with simultaneous presence of spheroids, insert of G) or mild axonal injury with intact axons in a +cMOG co-immunized animal (insert of H). * denotes p<0.05, * p<0.001. Data are displayed as mean ± standard error of the mean (SEM)

2.3. Binding mode of l-MOG$_{35-55}$ and c-MOG$_{35-55}$ peptides in complex wih murine MHC class II (H2-IA^b)

A number of studies have identified the mode of binding of l-MOG$_{35-55}$ to murine MHC class II, H2-IA^b.[27, 28] It was noted that the amino acids in MOG$_{38-51}$ peptide were important for binding to H2-IA^b. Residues R^{41}, F^{44}, R^{46} and V^{47} constituted the major T cell receptor contact residues since Ala substitutions abrogated T cell responses without affecting the binding affinity of the peptide to H2-IA^b;[27] G38 and W39 act as minor T cell receptor binding residues. In addition, Y^{40} was identified to be important in anchoring the peptide to H2-IA^b, which occupies pocket P1 of the commonly identified pockets of MHC complexes,[27] as Ala substitution at this residue decreaed the binding

affinity of the peptide to H2-IA^b up to 50 %. Considering this information for validation purposes, the l-MOG$_{35-55}$ sequence was examined for its positioning to the H2-IA^b using the IEDB server, which uses several algorithms for identifying positioning of antigens within MHC alleles (see materials and methods). The results showed a predicted higher affinity of the YRPPFSRVV sequence (MOG$_{40-48}$) than the CLIP$_{91-99}$ peptide that was used for comparison purposes as it has been co-crystallized with H2-IA^b (Table 1). This result, being in accordance with the aforementioned experimental results, showing that pockets P1-P9 are more probable to be occupied by the specific MOG$_{40-48}$ sequence, was used to build the models of the l-MOG$_{35-55}$ and c-MOG$_{35-55}$ interaction with H2-IA^b.

The 3-D complex models of l-MOG$_{35-55}$-H2-IA^b and c-MOG$_{35-55}$-H2-IA^b were consecutively built by amino acid replacement through homology modeling, in order to gain a better understanding of the elements of anchoring. The occupancy of pockets P1-P9 and the respective MOG$_{40-48}$ sequences is shown in Fig. 4. Pockets P1-P9 are occupied by residues Y$_{40}$RPPFSRV$_{48}$ respectively in both peptides, l-MOG$_{35-55}$ and c-MOG$_{35-55}$. In the case of l-MOG$_{35-55}$ (Fig. 4a) Y^{40} occupies P1, forming electrostatic interactions between the hydroxyl group and E86*β*. P4 is occupied by P^{43} making hydrophobic interactions with F11*α*, V78*α* and a hydrogen bond with N62*α*. S^{45} interacts with N69α in P6 and V^{48} is located in a hydrophobic environment of P9 interacting with V72*α* and W61*β*. In the case of c-MOG (Fig. 4b), cyclization does not seem to interfere with the occupancy of pockets P1, P4, P6 and P9 similarly to our previous reported in smaller length cyclic APLs.[29] The topology of corresponding MOG$_{40-48}$ residues to pockets P1, P4, P6 and P9 is the same, as the 20 length cyclic peptide and has adequate backbone length to dock to the MHC class II. Residues N$_{53}$GK$_{55}$-M$_{35}$EV$_{37}$ point towards the TCR interaction site.

Based on the clinical and neuropathological data (approximately 50 % better clinical and histological outcomes), we may assume that c-MOG$_{35-55}$ (when animals are co-immunized with a 1:1 cyclic-linear emulsion) is antagonizing the linear peptide for induction of immune responses. We hypothesize that a peptide-specific antagonism (c-MOG$_{35-55}$ against l-MOG$_{35-55}$) is likely responsible for the beneficial effects of c-MOG$_{35-55}$ since c-MOG$_{35-55}$ confers a similar binding affinity consensus and affinity with l-MOG$_{35-55}$ to H2-IA^b (Table 1). In addition, as c-MOG$_{35-55}$ binds within the H2-IA^b binding groove the TCR contact residues are different to that of l-MOG$_{35-55}$, hence it could lead to T cell antagonism. The data of co-immunization with c-MOG$_{35-55}$ have been replicated in 2 experimental sets (acute and chronic). This increases the validity of the data, as a prerequisite according to ARRIVE criteria.[30]

Table 1

Highest ranked peptides using the consensus approach for prediction of peptide binding affinity to the H2-IA^b allele on the free epitope database and prediction resource (IEDB). Peptides are ranked (Rank percentage) using the consensus method.

Peptide	**Residue positioning** 123456789	**SMM-align predicted IC_{50} (nM)**	**NN-align predicted IC_{50} (nM)**	**% Rank**
MOG_{40-48} (linear, cyclic)	YRPPFSRVV	72	15.50	0.28
MBP_{87-95}	YRPPFSRVV	236	79.40	1.78
$CLIP_{91-99}$ (control)	MRMATPLLM	2113	281	10.90

NN-align, an artifical neural network-based alignment algorithm for MHC class II peptide binding prediction; SMM-align, stabilization matrix alignment method for prediction of MHC class II binding affinity.

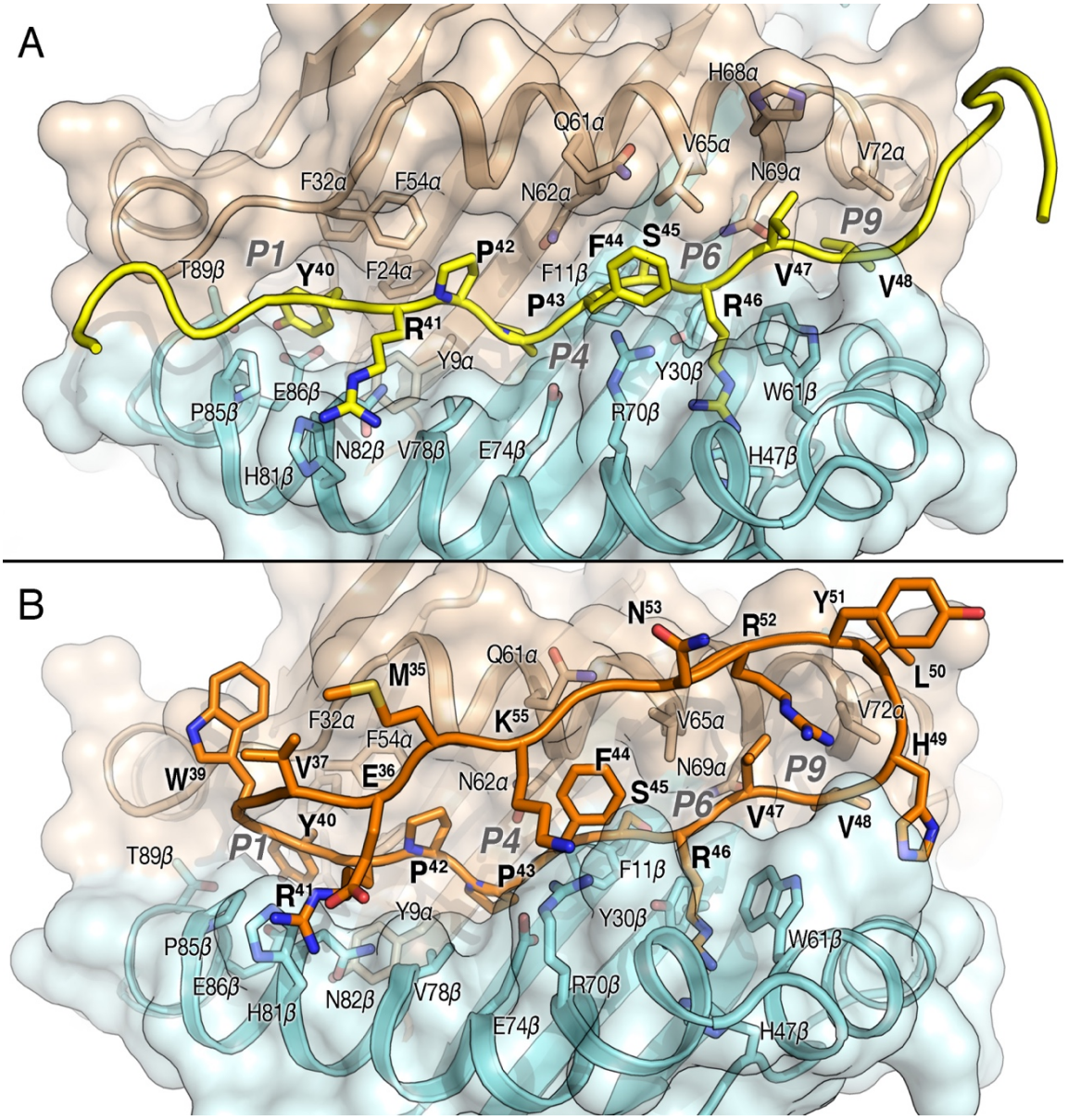

Fig. 4. Ribbon and surface representations of (A) l-MOG$_{35-55}$ (in yellow) and (B) c-MOG$_{35-55}$ (in orange) peptides bound to the modeled H2-IA^{b}. Chains *α* and *β* are shown in wheat and cyan colors respectively. Peptide numbering is shown in bold letters.

*2.4. Binding studies of l-MOG$_{35-55}$ and c-MOG$_{35-55}$ peptides in complex with human HLA-DR2 (DRB1*1501)*

2.4.1. Both l-MOG$_{35-55}$ and c-MOG$_{35-55}$ bind to HLA-DR2.

In order to determine the binding ability of l-MOG$_{35-55}$ and c-MOG$_{35-55}$ peptides to HLA-DR2 *in vitro*, competition assays were used based on a gel filtration method as previously published.[17, 31-36] MBP$_{83-99}$-AMCA-labeled peptide and immunoaffinity purified HLA-DR2 isolates from EBV transformed human DRB1*1501 B cell lines. As competitors l-MOG$_{35-55}$ and c-MOG$_{35-55}$ peptides were used in different concentrations, MBP$_{83-99}$ was used as a positive control. Linear MOG$_{35-55}$ bound with high affinity similar to that of control MBP$_{83-99}$ peptide and c-MOG$_{35-55}$ peptide bound with reduced binding capacity to HLA-DR2 but still with considerable affinity (Fig. 5)

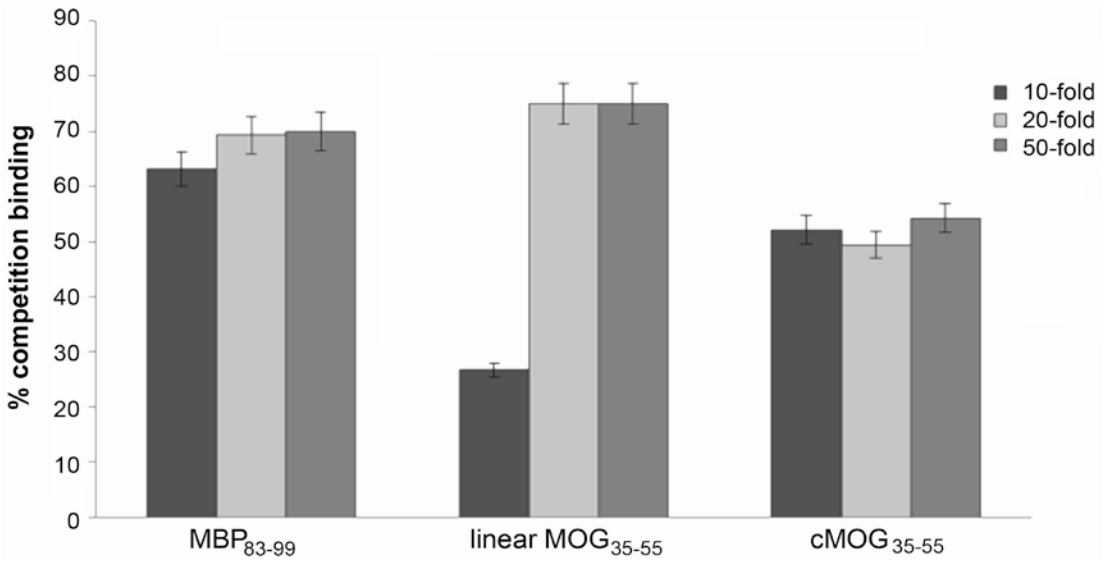

Fig. 5. Binding of l-MOG$_{35-55}$ and c-MOG$_{35-55}$ peptides to HLA-DR2. Competition binding of MBP$_{83-99}$ AMC-labelled peptide with 10-fold, 20-fold or 50-fold (M) excess of MBP$_{83-99}$, l-MOG$_{35-55}$ or c-MOG$_{35-55}$ peptides. % competition is shown on the y-axis and peptides are labeled on the x-axis. The experiments were done in triplicate and the results are given as mean ± standard error of the mean (SEM).

2.4.2. c-MOG$_{35-55}$ adopts a similar conformation to linear MBP$_{83-99}$

In order to assess the data of l-MOG$_{35-55}$ and c-MOG$_{35-55}$ peptide binding to HLA-DR2, MOG$_{35-55}$ sequence was examined for its positioning to the HLA-DR2 using the IEDB server, compared to MBP$_{83-98}$ sequence (Table 2). From the peptides affinity prediction, the optimal predicted binding sequence for l-MOG$_{35-55}$ is F_{44}SRVVHLYR_{52}. What was remarkable to find is that, the resulting MOG$_{35-55}$ sequence in the cyclic peptide, contains a highly homologous sequence to MBP$_{83-99}$ due to the cyclic nature produced by the fused termini. Specifically, the highest scored sequence of cMOG, MOG$_{[(48-55)-(35)]}$ (brackets denote the linear sequence parts in the context of a cyclic peptide) V_{48}HLYRNGK_{55}-M_{35}, is homologous to the MBP$_{87-95}$ P1-P9 occupying residues V_{87}HFFKNIVT_{95}.[37, 38] Comparing the two sequences residues occupying pockets P1, P2 and P6 are identical (V, H, N respectively) and pockets P3, P4 and P5 have similar corresponding residues (F/L, F/Y and R/K respectively). The MOG$_{[(48-55)-(35)]}$ sequence was predicted to have similar affinity to MBP$_{87-95}$ and considerably higher that MOG$_{44-52}$ in all three used algorithms.

To assess the binding prediction results, models of the peptides in complex with HLA-DR2 were generated using homology modeling. Fig. 6 depicts the crystal complex of HLA-DR2 with MBP$_{83-98}$ and the modeled complexes with l-MOG$_{35-55}$ and c-MOG$_{35-55}$. HLA-DR2 has a highly hydrophobic P1 pocket formed by F24*α*, F32*α*, V85*β* and V86*β*, in which V^{87} of MBP$_{83-98}$ is positioned (Fig. 6a). F^{90} of MBP$_{83-98}$ is located in pocket P4, comprised of R13*β*, F26*β*, Q70*β* and Y78*β*, N^{92} interacts with E11*α* and R13*β* in P6 and T^{95} is located between I71*α* and D57*β*. In the case of l-MOG, F^{44} and V^{47} occupy hydrophobic pockets P1 and P4 respectively (Fig. 6b). H^{49} is positioned in P6 and R^{52} is buried deep in P9, probably forming a strong salt bridge with the D57*β* side chain. For c-MOG$_{35-55}$, as mentioned before, the MOG$_{[(48-55)-(35)]}$ sequence that occurs after cyclization is highly homologous to MBP$_{87-95}$ (Table 2) and was therefore expected to have a very similar interaction pattern (Fig. 6c). Indeed, the model complex showed the exact same topology for residues V^{48}, H^{49} and Y^{51} compared to MBP$_{87-95}$ V^{87}, H^{88} and

F^{90} occupying pockets P1, P2 and P4 respectively. R^{52} in P5 looses its extended side chain conformation pointing to TCR, due to the cyclization steric overlap with c-MOG_{35-55} backbone. Lastly, M^{35} occupies P9, mainly interacting with I^{72}. The binding conformational data confirms that even though c-MOG_{35-55} is a weaker binder to its linear counterpart, l-MOG_{35-55} (due to the cyclization effects) it still has considerable affinity to HLA-DR2 (Fig. 5).

Table 2

Highest ranked peptides using the consensus approach for prediction of peptide binding affinity to HLA-DR2 (DRB1*1501) allele on the free epitope database and prediction resource (IEDB). Sequences in brackets denote the cyclic nature of the peptide. Peptides are ranked (Rank percentage) using the consensus method.

Peptide	Residue positioning 123456789	SMM-align predicted IC_{50} (nM)	NN-align predicted IC_{50} (nM)	Sturniolo score	% Rank
MBP_{87-98} (control)	VHFFKNIVT	22	12.60	6	0.10
$MOG_{[(48-55)-(35)]}$ (cyclic)	VHLYRNGKM	135	27.40	5.08	1.93
MOG_{44-52} (linear)	FSRVVHLYR	528	57.90	2.80	5.94

NN-align, an artifical neural network-based alignment algorithm for MHC class II peptide binding prediction; SMM-align, stabilization matrix alignment method for prediction of MHC class II binding affinity; Sturniolo score, a prediction software that scans tissue-specific and promiscuous HLA class II peptide databases using DNA microarrays and virtual HLA class II matrices

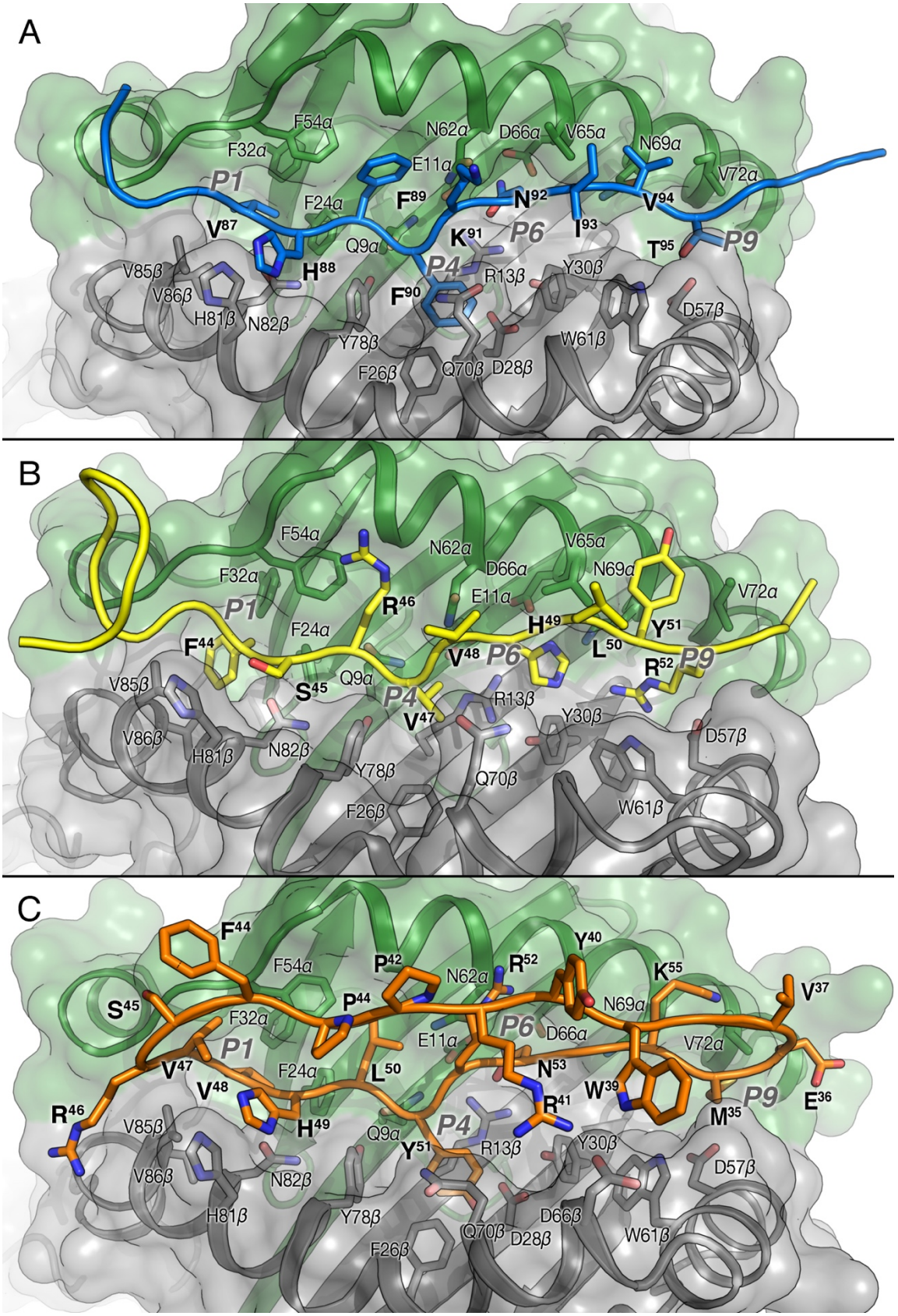

Fig. 6. Ribbon and surface representations of the (A) MBP_{83-99} (in blue) - HLA-DR2 crystal structure [37] and model complexes of (B) l-MOG_{35-55} (in yellow) and (C) c-MOG_{35-55} (in orange) peptides bound to HLA-DR2. Chains *α* and *β* are shown in green and gray colors respectively. Peptide numbering is shown in bold letters.

3. Conclusion

Our proof-of-concept studies support our hypothesis that co-administration of a c-MOG_{35-55} peptide at a 1:1 ratio with the corresponding l-MOG_{35-55} peptide during the induction of EAE ameliorates its clinical course. This is reflected to reduced clinical severity of the acute phase as well as reduced overall disease burden. Such clinical effects result from the ameliorated inflammatory, axonopathic and demyelinating processes within the CNS of the treated animals. The benefit in inflammatory processes is maintained during both acute and chronic phases of EAE. The same is also evident for the demyelinating processes. Axonopathy is also significantly reduced during the acute phase of the disease and this results to an important white matter tract preservation during the chronic phase of EAE. Importantly, the conserved myelination and axonal integrity of spinal cord tracts in animals co-immunized with c-MOG_{35-55} peptide are reflected to significantly ameliorated chronic neurological deficits in these animals, compared to controls.

Our data from the modeling and binding studies provide a further insight on such a beneficial effect of c-MOG_{35-55} on EAE. Although c-MOG_{35-55} binds to mouse (H2-IA^b) and human (HLA-DR2) MHC class II molecule, it has lower affinity to its linear counterpart (l-MOG_{35-55}) and to control agonist peptide MBP_{83-99}. At the same time, the binding of c-MOG_{35-55} to HLA-DR2 results in a somewhat different amino acid contact to the TCR which could potentially result in TCR antagonism and thus explain part of the beneficial effects on EAE. Eventually, this novel peptide (c-MOG_{35-55}) could possibly be conjugated to an appropriate carrier (ie. mannan, targeting antigen presenting cells) to result in a novel immunomodulatory treatment of human MS where l-MOG_{35-55} autoimmunity plays a role in the pathogenesis of disease.[19-21, 23-25]

4. Experimental section

4.1. Solid-phase peptide synthesis of cyclic-MOG_{35-55}

Linear protected $MOG_{\mathbf{35-55}}$ (rat, mouse) (H_2N-Met^{35}-Glu-Val-Gly-Trp-Tyr-Arg-Ser^{42}- Pro-Phe-Ser-Arg-Val-Val-His-Leu-Tyr-Arg-Asn-Gly-Lys^{55}-OH) was synthesized on 2- chlorotrityl chloride resin (CTLR-Cl) using the Fmoc/tBu methodology (Scheme 1). All amino acids were purchased from CBL (Patras, Greece). Peptide synthesis was on a 0.5 mmol scale up to the final protected analog. The use of the 2-chlorotrityl resin under mild conditions (DCM/TFE, 7/3) for cleaving the peptide-resin bond, allowed the release of high yield and purity of the protected peptide from the resin. Yield of fully protected peptide-resins was > 90 %.

Cyclization of linear protected $MOG_{\mathbf{35-55}}$ was achieved using O-benzotriazol-1-yl-N,N,N',N'-tetramethyluronium tetrafluoroborate (TBTU) and 1-hydroxy-7-azabenzotriazole, 2,4,6 collidine in DMF solution, allowing fast reactions and high yield cyclization products (Scheme 2). The cyclization reaction was monitored using the ninhydrin test, and the reaction mixture was resolved by thin-layer chromatography, nbutanol/acetic acid/water (4/1/1) solvent system and analytical HPLC in C4 Nucleosil RP column 5nm packing material. The protected cyclic analog was then released from side chain protected groups with 90 % trifluoroacetic acid (TFA) in DCM solution containing 5 % Dithiothreitol/water/Anisole as scavengers. Purification of the final cyclic peptide analog was accomplished with the use of a Waters Delta Prep

HPLC chromatography system equipped with a Prep LC controller and a Waters 2996 Photodiode array detector. Separation was achieved on Nucleosil RP-18 reverse phase column with a 7 µm pack material with a stepped linear gradient of acetonitrile in 0.1 % CF_3CO_2H at a flow rate of 8ml/min. Cyclic analogue, 5 mg per sample was injected for the collections of the fractions according to the chromatogram data. Elution of the peptide analogue was detected form the absorbance at 254 nm and 230 nm simultaneously. The fractions containing the required peptide were pooled following removal of CH_3CN on a rotary evaporator at 40 °C and lyophilized. The final cyclic peptide was > 98 % pure as analyzed by analytical RP-HPLC and ESI-MS (Fig. 7).

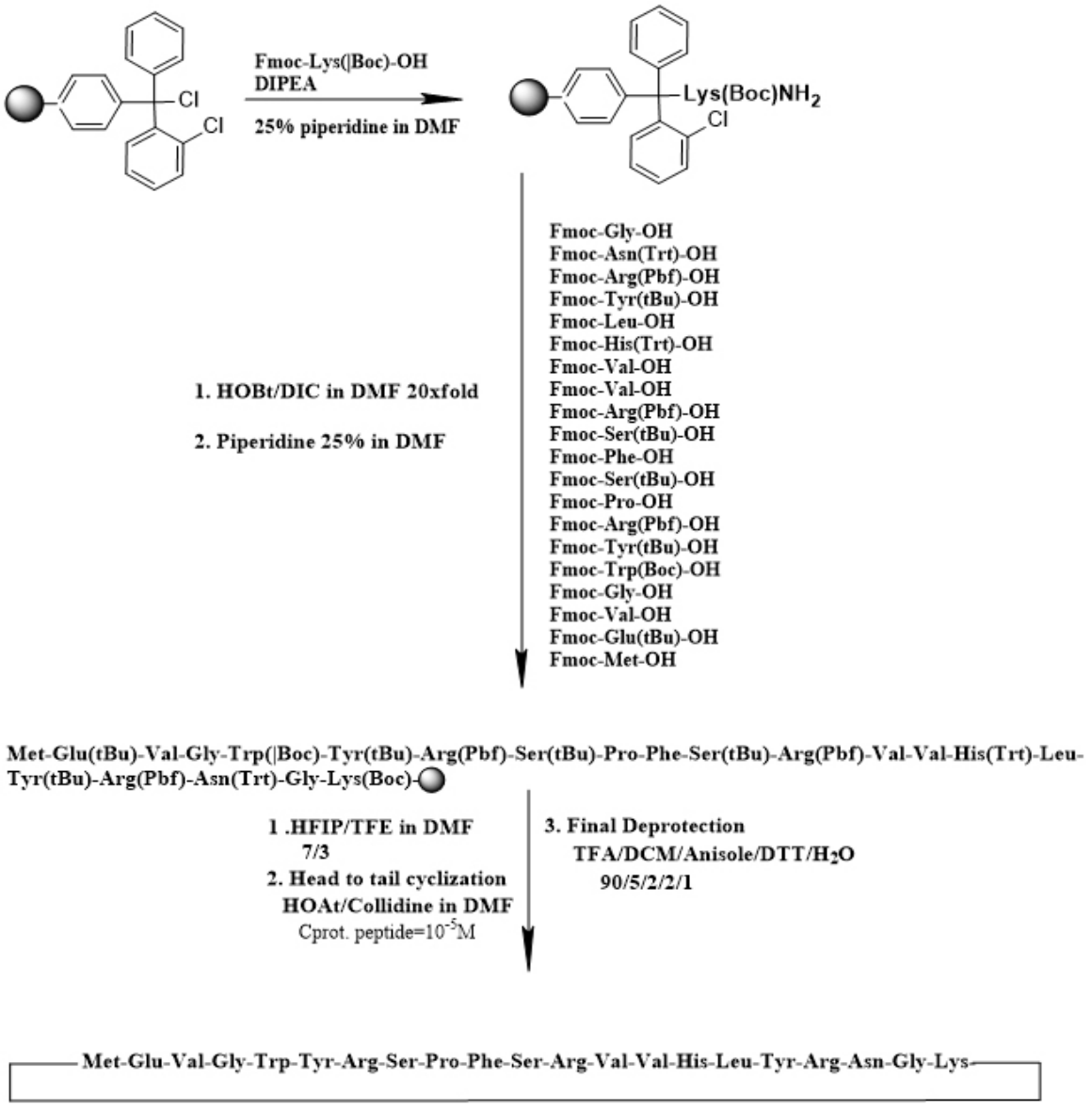

Scheme 1: Schematic representation of chemical synthesis of c-MOG_{35-55} peptide

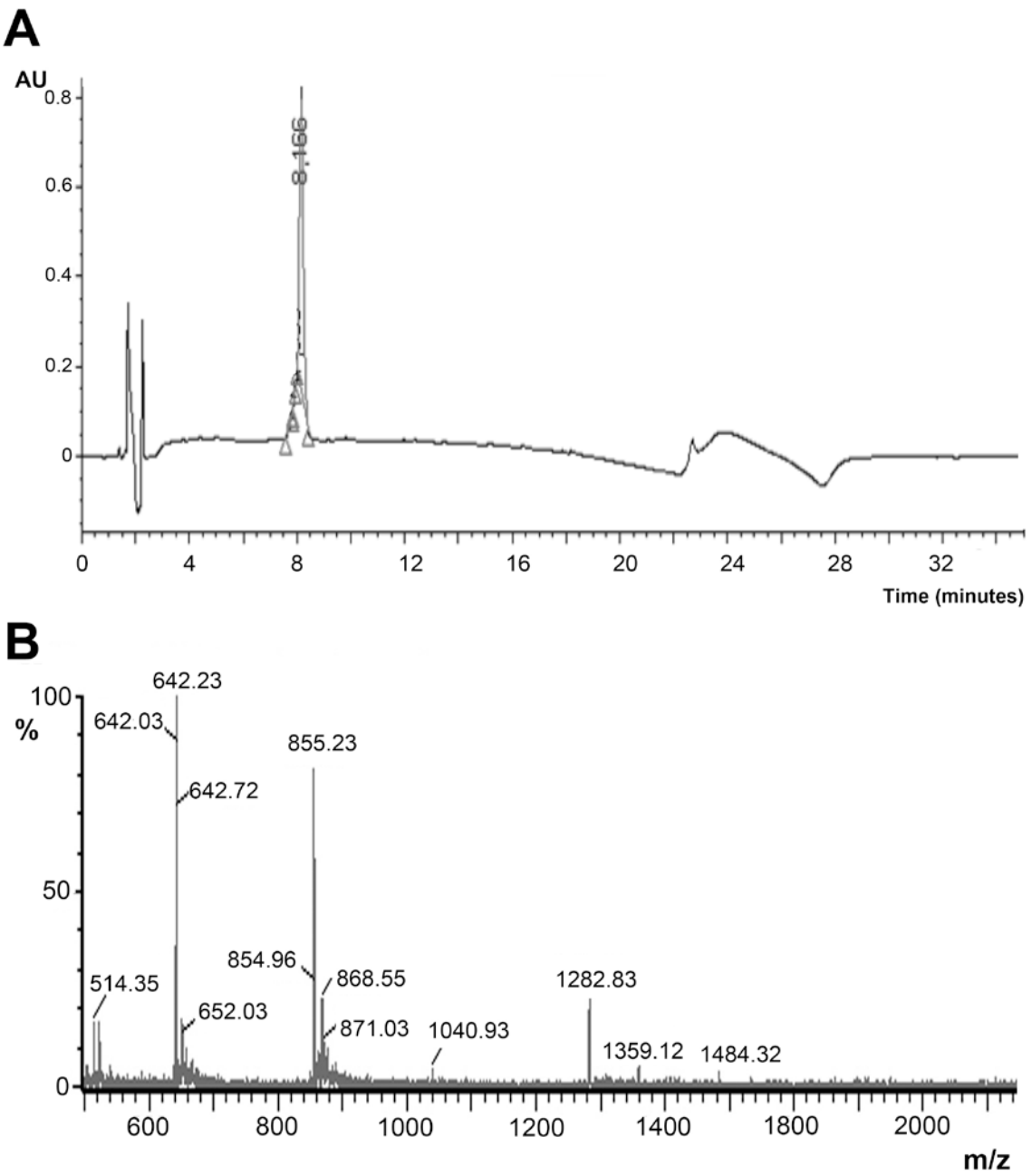

Fig. 7. (A) Analytical RP-HPLC of purified (purity > 98 %) c-MOG$_{35-55}$ peptide. Column: Xbridge C18, 150mm×4.6 mm, 3.5μm packing (Part/N= 186003034). RT: 9.49min Conditions: gradient 5% (B)-100% (B), in 30 min, flow rate 1 mL/min. [Eluents (a): solution TFA in H_2O 0.1% (v/v), (b): solution TFA in AcN 0.1% (v/v)]. (B) ESI+MS of c-MOG$_{35-55}$ peptide. M +2H$^+$/2: 1282.83, M +3H$^+$/3: 855.23. M +4H$^+$/4: 642.23].

4.2. Animal handling

Female C57BL/6 pathogen-free mice were purchased from Hellenic Pasteur Institute, Athens, and housed in the animal facility of the B' Neurological Department of the AHEPA University Hospital, Aristotle University Medical School in accordance with the National Institute of Health guidelines. Mice were fed a regular diet and given water without antibiotics.

4.2.1. EAE induction and evaluation of clinical disease

MOG EAE was induced as we previously described.[39, 40] Briefly, female C57BL/6 10 weeks-old mice, were divided into different groups depending on the peptides used. Control groups in all experiments were injected with 300 μg of linear-MOG_{35-55} or c-MOG_{35-55} peptides (mouse, rat) (synthesized by the group of Prof. Matsoukas). Mice were also immunized using a 1:1 mixture of the linear $MOG_{35–55}$ peptide together with cyclic MOG_{35-55} (c-MOG_{35-55}). All groups were injected subcutaneously (sc) at the left para-lumbar region of emulsions composed of the specific peptide mixture diluted in 100 μl filtered phosphate buffered saline (PBS) and emulsified with 100 μl complete Freund's adjuvant (CFA) with 4 mg/ml *Mycobacterium tuberculosis* H37RA, to a total injected volume of 200μl (day 0). Additionally, on day of induction (day 0), all groups were also given intraperitoneally (ip) 400 ng of pertussis toxin (Sigma) diluted in 0.5 ml of filtered PBS. On day 2, a further 200 ng of pertussis toxin was injected ip. A second injection of the emulsified peptides, was also delivered 7 days later into the right para-lumbar region.

Three experiments were conducted using exactly the same experimental procedures: (i) chronic EAE, mice were sacrificed at day 46 post disease induction; (ii) acute EAE, mice were sacrificed at day 17 post disease induction, and, (iii) comparison between the immunogenic properties of c-MOG_{35-55} versus linear MOG_{35-55}. All mice were examined daily and evaluated for body weight changes and clinical signs of disease. The clinical status of the mice was graded as follows: 0, without clinical disease; 1, flail tail; 2, tail paralysis; 3, hind limb weakness sufficient to impair righting; 4, paraplegia; 5, paraplegia with forelimb paresis or plegia; 6, death from EAE.

4.3. Histopathology

On acute (day 17) and chronic (day 46) phase of EAE, mice were subjected to transcardial perfusion with 4 % paraformaldehyde in PBS (pH 7.2, ice cold). Brains and spinal cords were removed, post-fixed in the same fixative for approximately 20 hours, routinely processed for paraffin embedding and sectioned at 6 μm. Sections from mice of acute and chronic phases of the disease, were then stained using the following methods: (i) a modified Bielschowsky silver (BLS) impregnation staining method combined with haematoxylin (Hem) (BLS+Hem), for the simultaneous evaluation of axonal injury, axonal loss and inflammatory processes in EAE as previously described;[41] (ii) Luxol fast blue (LFB) staining counterstained with Nuclear fast Red for the detection of demyelinating areas within the CNS of mice, using routine histopathological protocols.

Pathological evaluation was performed under a light microscope (Olympus Axioplan-2) by two blinded investigators and photos were taken using a CCD camera (Nikon). Five randomly selected longitudinal sections per tissue (brains and spinal cords) were evaluated as follows: for each animal, each section was evaluated under 20x or 40x optical fields (depending on the object of study) so as to cover the entire area of the section. Data were expressed per mm^2 of tissue, where appropriate. Spinal cords had the majority of lesions (compared to brains), therefore pathological studies were focused on the spinal cord sections of the animals.

Depending on the evaluated parameter we used the following scales as previously described.[39, 42] Axonal injury (AI), was evaluated using the following scale: 0 = no AI, 1+ = scattered dystrophic injured axons without any spheroid or ovoid, 2+ = mild AI with the presence of at least one spheroid or ovoid, 3+ = moderate AI, 4+ = severe AI; generally injured axons were defined and identified as spheroids and ovoids

(which represent axonotmesis), and dilated (dystrophic) axons which represent injured axons not yet being cut. Axonal loss (AL) was evaluated using the following scale: 0 = normal axonal density, 1+ = <25 % AL, 2+ = mild AL (26-50 %), 3+ = moderate to severe (51-75 %) AL, 4+ = severe AL (>75 %); various degrees of decreased density of axons was attributed to axonal loss and evaluated accordingly. Tissue infiltrations were evaluated under a 20x objective and data were expressed as the number of infiltrating cells per mm^2 and number of infiltrating cells per infiltration. The demyelination of white matter was evaluated under 40x optical fields: using a prefrontal grid, we measured the area of demyelination and the total area of white matter in each optical field and then calculated the % of demyelination.

4.4. Statistical analysis

Statistical analysis of mouse data was performed using the SPSS 23.0 software. For scale clinical and histopathological data, normality of distribution was tested using Shapiro-Wilk tests. For 2 group comparisons we applied either Student's *t*-test (parametric data) or Mann-Whitney U test (non-parametric data). For nominal or ordinal data and comparisons between 2 groups we used Pearson chi-square or Fisher's exact tests, where appropriate. Kaplan-Meier survival analysis was used for the clinical course of EAE, with "disease onset" as the end-point of the analysis (day of disease onset, dDO, was defined as the first day with clinical score of "1"). Mean Maximal Score (MMS) was calculated for each group using the maximal scores from each animal of each group. Disease burden was expressed as the Area Under the Curve (AUC), which was calculated for each mouse using the formula:[43]

$$\mathrm{AUC} = \left(\frac{\mathrm{score}_1}{2}\right) + \left(\sum_{i=2}^{k-1} \mathrm{score}_i\right) + \left(\frac{\mathrm{score}_k}{2}\right)$$

Data are expressed as mean±SEM, unless stated otherwise.

4.5. Competition binding of linear and cyclic MOG_{35-55} to HLA-DR2 allele

Binding of l-MOG_{35-55} and c-MOG_{35-55} analogs to HLA-DR2 was performed as previously demonstrated.[34, 35] Briefly, EBV transformed homozygous human B cell lines HTC-Lan (DRB1*1501, DRB5*0101) were used for isolating MHC class II molecule. HTC-Lan cell pellets were lyzed by nonidet P-40 and HLA-DR2 isolated from homogenates by affinity chromatography using the monoclonal antibody L243. The purity of the preparation was checked by SDS-PAGE, HPSEC and western blotting (not shown). Competition binding assays concerning linear MOG_{35-55} and c-MOG_{35-55} were carried out using Fluorescent AMCA-labelled allele-specific MBP_{83-99} for HLA-DR2b chain. Solubilized HLA-DR2 (0.66 mM) was incubated for 48 h at 37 ^oC with MBP_{83-99}-(AMCA)-labeled peptide dissolved in 150 mM sodium phosphate, pH 6.0, containing 15 % acetonitrile, 0.1 % Zwittergent-12 (Calbiochem). Competition assays were performed in a 1 μM solution of AMCA peptide. All samples were analyzed on a Pharmacia Superdex 75 HR 5/20 high performance gel filtration column. The column was operated at a flow rate of 0.3 ml/min using the HPSEC buffer, pH 6.0. The eluent passed through a Shimadzu fluorescence spectrometer (350/450 nm) and a Merck ultraviolet detector (214 nm) set in series. Fluorescence and UV signals eluting with the HLA-DR dimers were recorded by a model D 2500 integrator (Merck-Hitachi).

4.6. Docking studies of the HLA complexes

The peptides were evaluated for their potential affinity using the consensus approach for prediction of peptide MHC class II binding affinity (CONSENSUS) on the Free epitope database and prediction resource (IEDB). Peptides were evaluated in the IEDB analysis resource using the SMM-align,[44] NN-align[45] Sturniolo,[46] and the Consensus[47] algorithms. Using this procedure, for each peptide, a percentile rank for each of the three methods is generated by comparing the peptide's score against the scores of five million random 15-mers selected from SWISSPROT database. The MOG_{35-55} and $MOG_{[45-55]-[35-44]}$ (considering cyclization) peptides were evaluated for binding to allele H2-IA^b using $CLIP_{91-99}$ as control and to allele DRB1*1501 (HLA-DR2) using MBP_{82-99} as control.

4.7. Model preparation of linear and cyclic MOG_{35-55} in complex with murine H2-IA^b and human HLA-DR2.

Production of the model complexes was made by homology modeling using MODELLER 9.17,[48] using the crystal structures of HLA-DR2b complexed with MBP_{83-96} (pdb code 1BX2)[37] and H2-IA^b (pdb code 1MUJ)[49] as templates. Linear MOG_{35-55} and c-MOG_{35-55} (mouse, rat) peptides were aligned to the aforementioned crystalized peptides according to the docking results and positional restraints were applied to the protein. The overall stereochemical quality of the final models was evaluated by visual inspection and the discrete optimized energy (DOPE).[50] Cyclization for MOG_{35-55} peptides was performed manually by joining the C- and N- terminal residues, followed by an energy minimization of the whole complex by means of the conjugate gradient algorithm for 1000 steps in Discovery Studio v3.5.[51] For the linear MOG_{35-55} complexes, the same energy minimization parameters were used.

Acknowledgements

We would like to thank Prof. Leonardo Pardo for the software and CPU time provided for the computational studies. M-TM was supported in part by an IKY fellowship of excellence for postgraduate studies in Greece - Siemens program. VA would like to thank Vianex SA Greece for support (Specific task agreement MS immunotherapeutics). VA and JM would like to thank Vianex SA Greece for their enthusiasm, support and helpful discussions regarding drug development and immunotherapeutics against MS.

Author contributions

AL was involved in experimental design, EAE induction, data acquisition and analysis, histopathological data acquisition and analysis, manuscript writing. AL and OT were involved in histopathological stainings. AG performed EAE experiments. M-TM performed the computational studies and GD synthesized the peptides and undertook the binding studies under the supervision of HK. NG, JM and VA discussed the project and planned experiments and supervision.

References

1. Steinman, L. Multiple sclerosis: a coordinated immunological attack against myelin in the central nervous system. *Cell* 1996, 85, 299-302.
2. Krogsgaard, M.; Wucherpfennig, K. W.; Cannella, B.; Hansen, B. E.; Svejgaard, A.; Pyrdol, J.; Ditzel, H.; Raine, C.; Engberg, J.; Fugger, L. Visualization of myelin basic protein (MBP) T cell epitopes in multiple sclerosis lesions using a monoclonal antibody specific for the human histocompatibility leukocyte antigen (HLA)-DR2-MBP 85-99 complex. *J Exp Med* 2000, 191, 1395-412.
3. Martin, R.; McFarland, H. F.; McFarlin, D. E. Immunological aspects of demyelinating diseases. *Annu Rev Immunol* 1992, 10, 153-87.
4. Ota, K.; Matsui, M.; Milford, E. L.; Mackin, G. A.; Weiner, H. L.; Hafler, D. A. T-cell recognition of an immunodominant myelin basic protein epitope in multiple sclerosis. *Nature* 1990, 346, 183-7.
5. Steinman, L.; Waisman, A.; Altmann, D. Major T-cell responses in multiple sclerosis. *Mol Med Today* 1995, 1, 79-83.
6. Berger, T.; Rubner, P.; Schautzer, F.; Egg, R.; Ulmer, H.; Mayringer, I.; Dilitz, E.; Deisenhammer, F.; Reindl, M. Antimyelin antibodies as a predictor of clinically definite multiple sclerosis after a first demyelinating event. *N Engl J Med* 2003, 349, 139-45.
7. Diaz-Villoslada, P.; Shih, A.; Shao, L.; Genain, C. P.; Hauser, S. L. Autoreactivity to myelin antigens: myelin/oligodendrocyte glycoprotein is a prevalent autoantigen. *J Neuroimmunol* 1999, 99, 36-43.
8. Kerlero de Rosbo, N.; Hoffman, M.; Mendel, I.; Yust, I.; Kaye, J.; Bakimer, R.; Flechter, S.; Abramsky, O.; Milo, R.; Karni, A.; Ben-Nun, A. Predominance of the autoimmune response to myelin oligodendrocyte glycoprotein (MOG) in multiple sclerosis: reactivity to the extracellular domain of MOG is directed against three main regions. *Eur J Immunol* 1997, 27, 3059-69.
9. Sun, J.; Link, H.; Olsson, T.; Xiao, B. G.; Andersson, G.; Ekre, H. P.; Linington, C.; Diener, P. T and B cell responses to myelin-oligodendrocyte glycoprotein in multiple sclerosis. *J Immunol* 1991, 146, 1490-5.
10. Wallstrom, E.; Khademi, M.; Andersson, M.; Weissert, R.; Linington, C.; Olsson, T. Increased reactivity to myelin oligodendrocyte glycoprotein peptides and epitope mapping in HLA DR2(15)+ multiple sclerosis. *Eur J Immunol* 1998, 28, 3329-35.
11. Kort, J. J.; Kawamura, K.; Fugger, L.; Weissert, R.; Forsthuber, T. G. Efficient presentation of myelin oligodendrocyte glycoprotein peptides but not protein by astrocytes from HLA-DR2 and HLA-DR4 transgenic mice. *J Neuroimmunol* 2006, 173, 23-34.
12. Rich, C.; Link, J. M.; Zamora, A.; Jacobsen, H.; Meza-Romero, R.; Offner, H.; Jones, R.; Burrows, G. G.; Fugger, L.; Vandenbark, A. A. Myelin oligodendrocyte glycoprotein-35-55 peptide induces severe chronic experimental autoimmune encephalomyelitis in HLA-DR2-transgenic mice. *Eur J Immunol* 2004, 34, 1251-61.
13. Grigoriadis, N.; Ben-Hur, T.; Karussis, D.; Milonas, I. Axonal damage in multiple sclerosis: a complex issue in a complex disease. *Clin Neurol Neurosurg* 2004, 106, 211-7.
14. Grigoriadis, N.; Grigoriadis, S.; Polyzoidou, E.; Milonas, I.; Karussis, D. Neuroinflammation in multiple sclerosis: evidence for autoimmune dysregulation, not simple autoimmune reaction. *Clin Neurol Neurosurg* 2006, 108, 241-4.
15. Bittner, S.; Afzali, A. M.; Wiendl, H.; Meuth, S. G. Myelin oligodendrocyte glycoprotein (MOG35-55) induced experimental autoimmune encephalomyelitis (EAE) in C57BL/6 mice. *J Vis Exp* 2014.
16. Degano, M.; Garcia, K. C.; Apostolopoulos, V.; Rudolph, M. G.; Teyton, L.; Wilson, I. A. A functional hot spot for antigen recognition in a superagonist TCR/MHC complex. *Immunity* 2000, 12, 251-61.
17. Deraos, G.; Chatzantoni, K.; Matsoukas, M. T.; Tselios, T.; Deraos, S.; Katsara, M.; Papathanasopoulos, P.; Vynios, D.; Apostolopoulos, V.; Mouzaki, A.; Matsoukas, J. Citrullination of linear and cyclic altered peptide ligands from myelin basic protein (MBP(87-99)) epitope elicits a Th1 polarized response by T cells isolated from multiple sclerosis patients: implications in triggering disease. *J Med Chem* 2008, 51, 7834-42.
18. Katsara, M.; Minigo, G.; Plebanski, M.; Apostolopoulos, V. The good, the bad and the ugly: how altered peptide ligands modulate immunity. *Expert Opin Biol Ther* 2008, 8, 1873-84.

19. Katsara, M.; Deraos, G.; Tselios, T.; Matsoukas, J.; Apostolopoulos, V. Design of novel cyclic altered peptide ligands of myelin basic protein MBP83-99 that modulate immune responses in SJL/J mice. *J Med Chem* 2008, 51, 3971-8.
20. Katsara, M.; Deraos, G.; Tselios, T.; Matsoukas, M. T.; Friligou, I.; Matsoukas, J.; Apostolopoulos, V. Design and synthesis of a cyclic double mutant peptide (cyclo(87-99)[A91,A96]MBP87-99) induces altered responses in mice after conjugation to mannan: implications in the immunotherapy of multiple sclerosis. *J Med Chem* 2009, 52, 214-8.
21. Katsara, M.; Deraos, S.; Tselios, T. V.; Pietersz, G.; Matsoukas, J.; Apostolopoulos, V. Immune responses of linear and cyclic PLP139-151 mutant peptides in SJL/J mice: peptides in their free state versus mannan conjugation. *Immunotherapy* 2014, 6, 709-24.
22. Katsara, M.; Matsoukas, J.; Deraos, G.; Apostolopoulos, V. Towards immunotherapeutic drugs and vaccines against multiple sclerosis. *Acta Biochim Biophys Sin (Shanghai)* 2008, 40, 636-42.
23. Katsara, M.; Yuriev, E.; Ramsland, P. A.; Deraos, G.; Tselios, T.; Matsoukas, J.; Apostolopoulos, V. A double mutation of MBP(83-99) peptide induces IL-4 responses and antagonizes IFN-gamma responses. *J Neuroimmunol* 2008, 200, 77-89.
24. Katsara, M.; Yuriev, E.; Ramsland, P. A.; Deraos, G.; Tselios, T.; Matsoukas, J.; Apostolopoulos, V. Mannosylation of mutated MBP83-99 peptides diverts immune responses from Th1 to Th2. *Mol Immunol* 2008, 45, 3661-70.
25. Katsara, M.; Yuriev, E.; Ramsland, P. A.; Tselios, T.; Deraos, G.; Lourbopoulos, A.; Grigoriadis, N.; Matsoukas, J.; Apostolopoulos, V. Altered peptide ligands of myelin basic protein (MBP87-99) conjugated to reduced mannan modulate immune responses in mice. *Immunology* 2009, 128, 521-33.
26. Tseveleki, V.; Tselios, T.; Kanistras, I.; Koutsoni, O.; Karamita, M.; Vamvakas, S. S.; Apostolopoulos, V.; Dotsika, E.; Matsoukas, J.; Lassmann, H.; Probert, L. Mannan-conjugated myelin peptides prime non-pathogenic Th1 and Th17 cells and ameliorate experimental autoimmune encephalomyelitis. *Exp Neurol* 2015, 267, 254-67.
27. Petersen, T. R.; Bettelli, E.; Sidney, J.; Sette, A.; Kuchroo, V.; Bäckström, B. T. Characterization of MHC- and TCR- binding residues of the myelin oligodendrocyte glycoprotein 38–51 peptide. *European journal of immunology* 2004, 34, 165-173.
28. Ben- Nun, A.; de Rosbo, N. K.; Kaushansky, N.; Eisenstein, M.; Cohen, L.; Kaye, J. F.; Mendel, I. Anatomy of T cell autoimmunity to myelin oligodendrocyte glycoprotein (MOG): Prime role of MOG44F in selection and control of MOG- reactive T cells in H- 2b mice. *European journal of immunology* 2006, 36, 478-493.
29. Apostolopoulos, V.; Deraos, G.; Matsoukas, M.-T.; Day, S.; Stojanovska, L.; Tselios, T.; Androutsou, M.-E.; Matsoukas, J. Cyclic citrullinated MBP 87–99 peptide stimulates T cell responses: Implications in triggering disease. *Bioorganic & Medicinal Chemistry* 2016.
30. Kilkenny, C.; Browne, W. J.; Cuthill, I. C.; Emerson, M.; Altman, D. G. Improving bioscience research reporting: the ARRIVE guidelines for reporting animal research. *PLoS Biol* 2010, 8, e1000412.
31. Deraos, G.; Rodi, M.; Kalbacher, H.; Chatzantoni, K.; Karagiannis, F.; Synodinos, L.; Plotas, P.; Papalois, A.; Dimisianos, N.; Papathanasopoulos, P.; Gatos, D.; Tselios, T.; Apostolopoulos, V.; Mouzaki, A.; Matsoukas, J. Properties of myelin altered peptide ligand cyclo(87-99)(Ala91,Ala96)MBP87-99 render it a promising drug lead for immunotherapy of multiple sclerosis. *Eur J Med Chem* 2015, 101, 13-23.
32. Halder, T. M.; Bluggel, M.; Heinzel, S.; Pawelec, G.; Meyer, H. E.; Kalbacher, H. Defensins are dominant HLA-DR-associated self-peptides from CD34(-) peripheral blood mononuclear cells of different tumor patients (plasmacytoma, chronic myeloid leukemia). *Blood* 2000, 95, 2890-6.
33. Matsoukas, J.; Apostolopoulos, V.; Kalbacher, H.; Papini, A. M.; Tselios, T.; Chatzantoni, K.; Biagioli, T.; Lolli, F.; Deraos, S.; Papathanassopoulos, P.; Troganis, A.; Mantzourani, E.; Mavromoustakos, T.; Mouzaki, A. Design and synthesis of a novel potent myelin basic protein epitope 87-99 cyclic analogue: enhanced stability and biological properties of mimics render them a potentially new class of immunomodulators. *J Med Chem* 2005, 48, 1470-80.
34. Max, H.; Halder, T.; Kalbus, M.; Gnau, V.; Jung, G.; Kalbacher, H. A 16mer peptide of the human autoantigen calreticulin is a most prominent HLA-DR4Dw4-associated self-peptide. *Human immunology* 1994, 41, 39-45.
35. Max, H.; Halder, T.; Kropshofer, H.; Kalbus, M.; Müller, C. A.; Kalbacher, H. Characterization of peptides bound to extracellular and intracellular HLA-DR1

molecules. *Human immunology* 1993, 38, 193-200.
36. Tselios, T.; Apostolopoulos, V.; Daliani, I.; Deraos, S.; Grdadolnik, S.; Mavromoustakos, T.; Melachrinou, M.; Thymianou, S.; Probert, L.; Mouzaki, A.; Matsoukas, J. Antagonistic effects of human cyclic MBP(87-99) altered peptide ligands in experimental allergic encephalomyelitis and human T-cell proliferation. *J Med Chem* 2002, 45, 275-83.
37. Smith, K. J.; Pyrdol, J.; Gauthier, L.; Wiley, D. C.; Wucherpfennig, K. W. Crystal structure of HLA-DR2 (DRA* 0101, DRB1* 1501) complexed with a peptide from human myelin basic protein. *The Journal of experimental medicine* 1998, 188, 1511-1520.
38. Hahn, M.; Nicholson, M. J.; Pyrdol, J.; Wucherpfennig, K. W. Unconventional topology of self peptide–major histocompatibility complex binding by a human autoimmune T cell receptor. *Nature immunology* 2005, 6, 490-496.
39. Lourbopoulos, A.; Grigoriadis, N.; Lagoudaki, R.; Touloumi, O.; Polyzoidou, E.; Mavromatis, I.; Tascos, N.; Breuer, A.; Ovadia, H.; Karussis, D.; Shohami, E.; Mechoulam, R.; Simeonidou, C. Administration of 2-arachidonoylglycerol ameliorates both acute and chronic experimental autoimmune encephalomyelitis. *Brain Res* 2011, 1390, 126-41.
40. Theotokis, P.; Touloumi, O.; Lagoudaki, R.; Nousiopoulou, E.; Kesidou, E.; Siafis, S.; Tselios, T.; Lourbopoulos, A.; Karacostas, D.; Grigoriadis, N.; Simeonidou, C. Nogo receptor complex expression dynamics in the inflammatory foci of central nervous system experimental autoimmune demyelination. *J Neuroinflammation* 2016, 13, 265.
41. Lourbopoulos, A.; Grigoriadis, S.; Symeonidou, C.; Deretzi, G.; Taskos, N.; Shohami, E.; Grigoriadis, N. Modified Bielschowsky silver impregnation combined with Hematoxylin or Cresyl Violet counterstaining as a potential tool for the simultaneous study of inflammation and axonal injury in the central nervous system. *Aristotle University Med J* 2007, 34, 31-39.
42. Gur-Wahnon, D.; Mizrachi, T.; Maaravi-Pinto, F. Y.; Lourbopoulos, A.; Grigoriadis, N.; Higazi, A. A.; Brenner, T. The plasminogen activator system: involvement in central nervous system inflammation and a potential site for therapeutic intervention. *J Neuroinflammation* 2013, 10, 124.
43. Fleming, K. K.; Bovaird, J. A.; Mosier, M. C.; Emerson, M. R.; LeVine, S. M.; Marquis, J. G. Statistical analysis of data from studies on experimental autoimmune encephalomyelitis. *J Neuroimmunol* 2005, 170, 71-84.
44. Nielsen, M.; Lundegaard, C.; Lund, O. Prediction of MHC class II binding affinity using SMM-align, a novel stabilization matrix alignment method. *BMC bioinformatics* 2007, 8, 1.
45. Nielsen, M.; Lund, O. NN-align. An artificial neural network-based alignment algorithm for MHC class II peptide binding prediction. *BMC bioinformatics* 2009, 10, 1.
46. Sturniolo, T.; Bono, E.; Ding, J.; Raddrizzani, L.; Tuereci, O.; Sahin, U.; Braxenthaler, M.; Gallazzi, F.; Protti, M. P.; Sinigaglia, F. Generation of tissue-specific and promiscuous HLA ligand databases using DNA microarrays and virtual HLA class II matrices. *Nature biotechnology* 1999, 17, 555-561.
47. Wang, P.; Sidney, J.; Kim, Y.; Sette, A.; Lund, O.; Nielsen, M.; Peters, B. Peptide binding predictions for HLA DR, DP and DQ molecules. *BMC bioinformatics* 2010, 11, 1.
48. Webb, B.; Sali, A. Comparative protein structure modeling using Modeller. *Current protocols in bioinformatics* 2014, 5.6. 1-5.6. 32.
49. Zhu, Y.; Rudensky, A. Y.; Corper, A. L.; Teyton, L.; Wilson, I. A. Crystal structure of MHC class II IA b in complex with a human CLIP peptide: prediction of an IA b peptide-binding motif. *Journal of molecular biology* 2003, 326, 1157-1174.
50. Shen, M. y.; Sali, A. Statistical potential for assessment and prediction of protein structures. *Protein science* 2006, 15, 2507-2524.
51. Accelrys. *Discovery Studio Modeling Environment*, 3.5; Accelrys: San Diego, CA, 2012.